

MARANGONI EFFECT IN MOLTEN SALTS AND SLAGS

Kusuhiro Mukai

Faculty of Engineering, Kyushu Institute of Technology, Japan

Synopsis:

Direct observations have clarified the occurrences of Marangoni effect in the following high temperature melts: 1) Vigorous surface tension driven flow induced by surface tension gradient due to the temperature gradient on the surface of liquid bridges of molten NaNO_3 , KNO_3 , etc. 2) Fast shrinking and spreading of slag droplet on liquid Pb in response to the rapid change in applied potential. 3) Characteristic slag film motion on the surface of solid SiO_2 induced by surface tension gradient due to the concentration gradient of SiO_2 on the film surface of PbO-SiO_2 and $\text{Fe}_t\text{O-SiO}_2$ slags, causing a local corrosion of solid SiO_2 at the slag surface.

Key Word: Marangoni effect; fluid dynamics; direct observation; surface tension gradient; liquid bridge; molten salt; slag droplet; slag film; local corrosion; solid silica

I. Introduction

Surface(or interfacial) tension difference or gradient on the surface(or interfacial) of liquid, for example, in the direction x , can change the motion of liquid due to the surface shear stress τ_s , written as,

$$\tau_s = \frac{d\sigma}{dx} = \frac{\partial\sigma}{\partial T} \cdot \frac{dT}{dx} + \frac{\partial\sigma}{\partial c} \cdot \frac{dc}{dx} + \frac{\partial\sigma}{\partial\psi} \cdot \frac{d\psi}{dx} \dots\dots\dots(1)$$

Equation (1) indicates that surface (or interfacial) tension gradient is caused by the gradients of temperature T , concentration c of the surface active component in the liquid and electric potential ψ at the interface between two liquids.

In hydrodynamics, the surface (or interfacial) tension difference or gradient participating in the above dynamics is called the Marangoni effect[1]. Motions of liquid induced by the Marangoni effect, which is called Marangoni flow or Marangoni convection, are most intensive at the surface or the interface. There the motion can effectively promote both the mass transport and heat transport across the interface. Liquid salts and slags generally have higher surface or interfacial tension than the liquids at room temperature such as water, which is favorable to the occurrence of Marangoni flow in these liquids. A certain amount of studies[2] in relation to the Marangoni effect have been reported, for example, in glass technology, metallurgy, space technology, etc. However, in order to clarify the contribution of the Marangoni effect to those technological phenomena under normal gravity on the earth, it is still now of particular importance at the present stage of surface chemistry at high temperatures to substantiate the actual occurrence of the Marangoni effect in the phenomena, distinguishing between the Marangoni convection and density convection induced by the gradients of temperature and/or concentration of the liquids.

Authors have directly observed the actual occurrences of the Marangoni effect under normal gravity in the following systems: 1) Marangoni convection of molten salts and slags due to temperature gradient[3],[4], 2) spreading and shrinking of slag droplets on the metal due to changes in applied potential[5], and 3) Marangoni flow of slag film due to

concentration gradient[6]-[11]. This paper describes briefly the results of these direct observations, some of which are presented in relation to technological problems.

2. Marangoni Convection in Small Liquid Bridges of Molten Salts and Slags Due to Temperature Gradient[3],[4]

Motions in small liquid bridges of molten salts and slags were directly observed using a novel hot-thermocouple technique[12], which can produce surface tension gradient due to temperature gradient on the free surface of the melts as predicted from Eq.(1).

As shown in Fig.1, a liquid bridge of NaNO_3 , 3 mm in length, is held between two platinum disks (3 mm in diameter) in the air. Each disk is welded on the tip of Pt-10%Rh - Pt-30%Rh thermocouple, which is used for both temperature measurement and heating. Temperature of one disk is kept at 640 K and that of the other is modulated between 620 K and 640 K (Fig. 1). Fine platinum powders are added in the melt, and their motions are recorded by VTR and a high speed camera.

When the temperatures of two disks are equal (Fig.1(a)), two roll cells, one in the upper part and the other in the lower part of the bridge are observed. The surface flows toward the middle part of the bridge, where the surface temperature is lowest (625 K). When the lower disk temperature is lowered down to 620 K (Fig.1(b)), the lower roll cell disappears, leaving a single large cell, in which surface flows downwards. When the upper disk temperature is lowered down to 620 K (Fig.1(c)), there appears also a single roll cell as shown in Fig.1(c) with reverse flow direction of Fig.1(b) and its surface flows upwards.

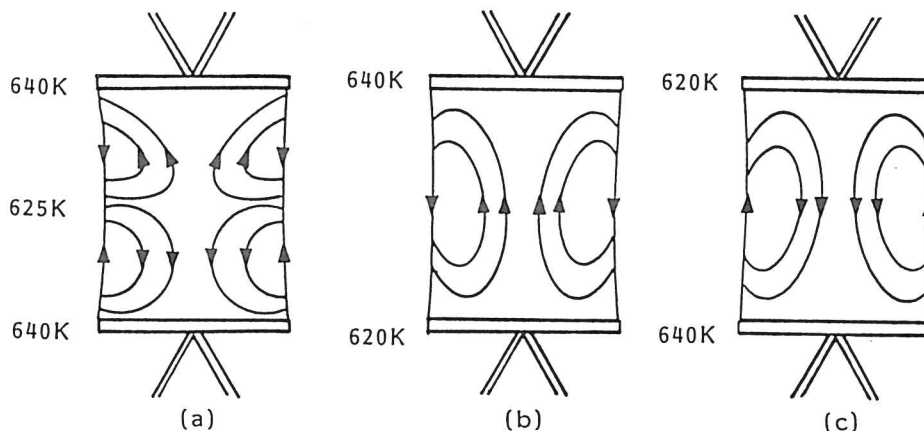


Fig.1 Schematic flow pattern of Marangoni convection in a liquid bridge of NaNO_3 under different temperature distribution.

Even when the free surface of the liquid bridge is maintained horizontally, principally the same liquid motions as those of Fig.1 were observed, although the shape of the liquid bridge is slightly changed from cylinder due to gravity.

Surface tension of NaNO_3 decreases with increasing temperature. Then, all of the convections in the liquid bridge shown in Fig.(1) are qualitatively explained to be caused by the Marangoni effect due to temperature gradient.

These liquid motions of NaNO_3 are simulated by a numerical calculation under the assumption that the motions are induced by the Marangoni effect only, neglecting the contribution of density convection[13]. The liquid bridge is approximated by an axisymmetric right cylinder. The fundamental equations consist of a pair of the Navier Stokes equation and a convective energy equation with the Boussinesq approximation except for the temperature dependent surface tension. These equations are discretized and solved by means of the SIMPLER method. The calculated liquid motion represents well the experimentally observed Marangoni convection. The calculated velocity at the free surface in the middle part of the bridge, 2.5 cm/s, is in fairly good agreement with the observed mean velocity of Pt particles, 3.0 cm/s, at and around the free surface in the middle part of the liquid bridge, measured by the aid of high speed camera.

Principally the same Marangoni convection as that of NaNO_3 was observed in the liquid bridges of KNO_3 , criolite, $\text{Na}_2\text{O}-\text{B}_2\text{O}_3$, $\text{Li}_2\text{O}-\text{B}_2\text{O}_3$ and $\text{Li}_2\text{O}-\text{SiO}_2$. Marangoni convection in the liquid bridge of NaOH shows rather different behaviour with the change of temperature from the above mentioned materials, which is to be presented at this Conference[14].

3. Fast Shrinking and Spreading of Slag Droplet on Liquid Metal in Response to the Rapid Change in Applied Potential[5]

Motions of a PbO-30mol%SiO₂ slag droplet on liquid Pb in response to the rapid change in applied potential were directly observed and recorded photographically. The slag droplet of 0.1g mass was suspended by a Pt-20%Rh wire above the liquid Pb which was held in a silica dish at 1073 K in Ar atmosphere. Immediately after the slag droplet was contacted with the liquid Pb, photographs were taken of the liquid slag-metal system (Fig.2).

When the applied potential φ between the Pb(working electrode) and the Pt-Rh wire (counter electrode) was changed from $\varphi = 0$ V to the cathodic mode, the slag droplet responded within a few seconds by reverting from a fast shrinking to a spreading configuration. This rapid change was recorded photographically and the visible angle α between the metal and slag shown in Fig.2 was measured from the film. The interfacial tension between the metal and slag, σ_{ms} , can be obtained from Eq.(2) using the observed values of α .

$$\sigma_{ms}^2 = \sigma_m^2 + \sigma_s^2 - 2\sigma_m\sigma_s\cos\alpha \quad (2)$$

where σ_m is the surface tension of the the metal and σ_s is the surface tension of the slag.

Thus obtained interfacial tension is shown in Fig.3 as a function of time in response to the rapid change in the potential.

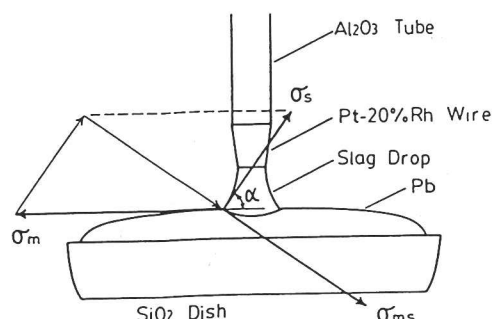


Fig.2 Diagrammatic representation of the visible angle α .

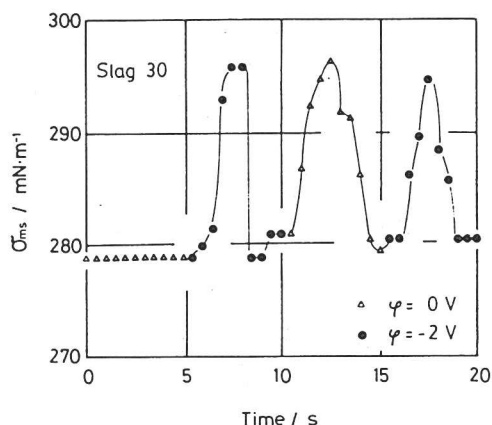


Fig.3 Calculated interfacial tension σ_{ms} as a function of time in response to changes in applied potential φ . PbO-30mol%SiO₂ slag.

The interfacial tension under an applied potential is affected by compositional changes due to electrode reactions and by changes in the applied potential itself, as shown by Lippmann's equation,

$$\left(\frac{\partial\sigma_{ms}}{\partial U}\right)_{T,p,\mu} = -q \quad (3)$$

where U is electrode potential, p is pressure, μ is chemical potential and q is surface density of the electric charge. During the measurement of σ_{ms} within 60 s after contacting the two liquids, the compositional change of the slag droplet is very small. Thus the change in σ_{ms} with φ in the present study must primarily be the result of the applied potential itself, that is the electrocapillarity phenomenon.

In Fig.3, zero time corresponds to approx. 15 s after contacting the two liquids with $\varphi = 0$ V. After 5 s of $\varphi = 0$ V the potential was changed to -2 V. The calculated σ_{ms} increased rapidly and reached a maximum at about 7.5 s and then decreased to a minimum before levelling off at a value almost equal to σ_{ms} at $\varphi = -2$ V as shown in Fig.4. Fig.4 was obtained from the measurement of σ_{ms} within 60 s after contacting the two liquid under constant applied potential by use of a potentiostat. After 5 s at -2 V, the voltage was again changed to $\varphi = 0$ V. The calculated σ_{ms} during this period went through another similar maximum and minimum and then levelled off to about the same value of σ_{ms} at the initiation of $\varphi = 0$ V at the 10 s position of Fig.3. This time variation of σ_{ms} can be qualitatively accounted for on the basis of the relation between σ_{ms} and φ . Fig.4 indicates that σ_{ms} must pass through a maximum when the potential is changed from $\varphi = 0$

to $\varphi = -2$ V or from $\varphi = -2$ to $\varphi = 0$ V.

The above experimental results and discussions indicate that the reversible fast motion of the slag droplet must primarily be caused by the Marangoni effect due to the change in applied potential as indicated from Eq. (1).

4. Slag Film Motion in Local Corrosion Zone of Solid Oxide

Direct observations have been made of the film motions of liquid PbO-SiO_2 and $\text{Fe}_2\text{O}_3\text{-SiO}_2$ slags in local corrosion zones for cylindrical and prism silica specimens.

4.1. $\text{SiO}_2(\text{s}) - (\text{PbO-SiO}_2)$ Slag System [6]-[10]

Immediately after immersing the SiO_2 specimen in the PbO-SiO_2 slag at 1073 K in Ar atmosphere, slag begins to creep up on the specimen surface to form slag film above the slag level. The slag film motion can be directly observed and recorded on a cinefilm by the aid of the movement of very small bubbles in the slag film. The slag film forms characteristic flow patterns, principally composed of wide zones of rising film and narrow zones of falling film, according to the contour of the specimen, as shown in Figs. 5 and 6.

In the case of cylindrical specimen, the position of the falling zone moves gradually on the surface of the specimen (Fig. 5). However, the prism specimen always has one zone of rising film at and around each corner of the specimen and one narrow zone of falling film at each plane side of the specimen as shown in Fig. 6.

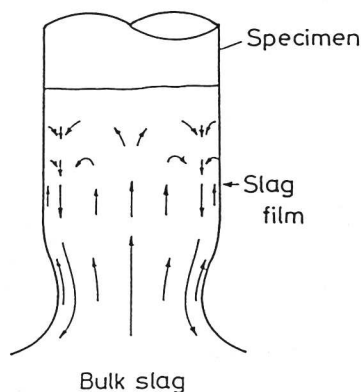


Fig. 5 Typical flow pattern of slag film on a cylindrical silica specimen 6 mm dia. immersed in PbO-SiO_2 slag.

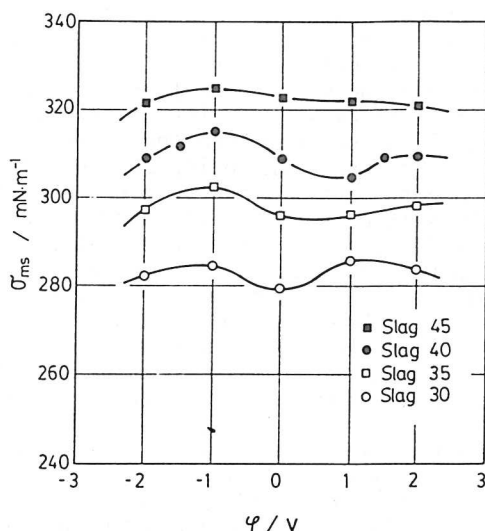


Fig. 4 Effect of applied potential φ on interfacial tension σ_{ms} . Slag i ($i=30, \dots, 45$) in the figure means i mol% SiO_2 in the slag.

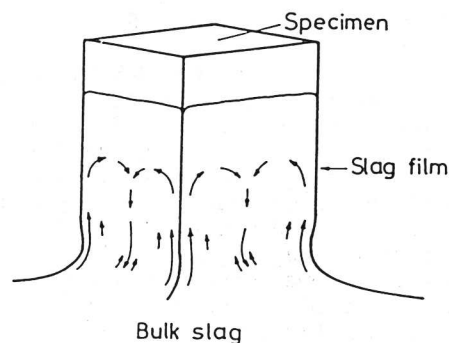


Fig. 6 Typical flow pattern of slag film on a prism silica specimen 6 mm square immersed in PbO-SiO_2 slag.

Films of the rising zone are several times thinner than those of the falling zone. Change in SiO_2 content in the solidified slag film is detected in the direction perpendicular to the specimen surface and also along the surface of the specimen in vertical direction.

Since contact time of the upper film with specimen is longer than the lower film, the upper film has higher SiO_2 content than the lower film due to the dissolution of SiO_2 from the specimen into the film. The difference in SiO_2 content causes a surface tension gradient in the vertical direction, for surface tension of PbO-SiO_2 slag increases with increasing SiO_2 content [15]. Thus the slag film is continuously pulled up by the surface tension gradient, that is, rising zone of the film is generated by the Marangoni effect due to concentration gradient as shown in Eq. (1). Since the film motion in the upper part of the specimen is slower than the lower part due to its high viscosity coefficient [16], the risen up slag is accumulated in the upper part. The thickened film caused by the accumulation begins to fall down when its weight exceeds the surface tension gradient, that

is, a falling zone of the film is formed.

Hydrodynamic analysis on the film motion, using the observed surface tension gradient along the surface of the film, results in good agreement between the calculated and observed film velocities. Velocity distribution in the slag film obtained from the analysis shows that the slag film motion in the local corrosion zone is still active even in a thin slag film with a thickness of several tens of μm (Fig.7). The film has concentration gradient of SiO_2 perpendicular to the surface of the solid silica, which means that a diffusion layer has been formed over the whole range of the slag film. The Marangoni flow in the slag film therefore results in breakdown of the diffusion layer, which is the main cause of local corrosion. In other words, the local corrosion proceeds largely as a result of the washing of the wall of solid silica with a fresh thin rising slag film induced by the Marangoni effect. The corner of a prism specimen that is continuously washed always by the rising film, as shown in Fig.6, is thus corroded much faster than the plane side, which leads to the formation of a round shape of horizontal cross section of the specimen from the initial square shape. On the other hand, a cylindrical specimen retains its initial round shape of horizontal cross section in the local corrosion zone, because the rising zone of the slag film shifts its location with time horizontally on the surface of the specimen, resulting in an almost even corrosion rate at the same level in the local corrosion zone.

4.2 $\text{SiO}_2(\text{s})-(\text{Fe}_t\text{O}-\text{SiO}_2)$ Slag System[11]

Surface tension of $\text{PbO}-\text{SiO}_2$ slag is increased by the component SiO_2 , as mentioned above, while SiO_2 decreases surface tension of $\text{Fe}_t\text{O}-\text{SiO}_2$ slag. The slag film motion in the local corrosion zone of this system could be also directly observed, because the major part of the local corrosion zone occurs in the meniscus region of the slag as shown in Fig.8. In this system, the slag film has two types of characteristic motion. One is a rotational motion around the specimen surface during the initial stage of the local corrosion of cylindrical specimen. Another is an up and down motion of the whole slag film all at once along the specimen surface during the developed stage of the local corrosion of cylindrical specimen, and during the whole stage of the corrosion of prism specimen. Corrosion rate at the corner of the prism specimen is $\sqrt{2}$ times as large as that at the plane. In a word, the cross section of the prism specimen keeps square during the whole stage of the corrosion, while in the system of $\text{SiO}_2(\text{s})-(\text{PbO}-\text{SiO}_2)$ slag, the horizontal cross section of the prism specimen changes its shape from square to round, as described in Sec.4.1. A mechanism of the local corrosion for the present system can be estimated

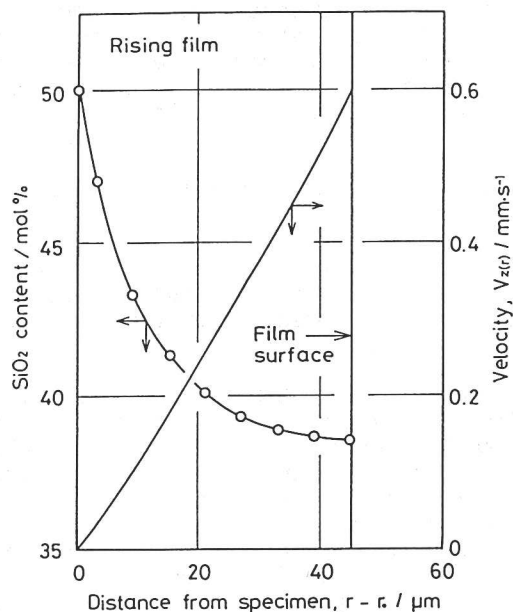


Fig.7 Distribution of vertical velocity, $V_z(r)$, and SiO_2 content in the slag film for a 6 mm dia. silica rod immersed for 0.3 ks in $\text{PbO}-30\text{mol}\%$ slag at 1073 K.

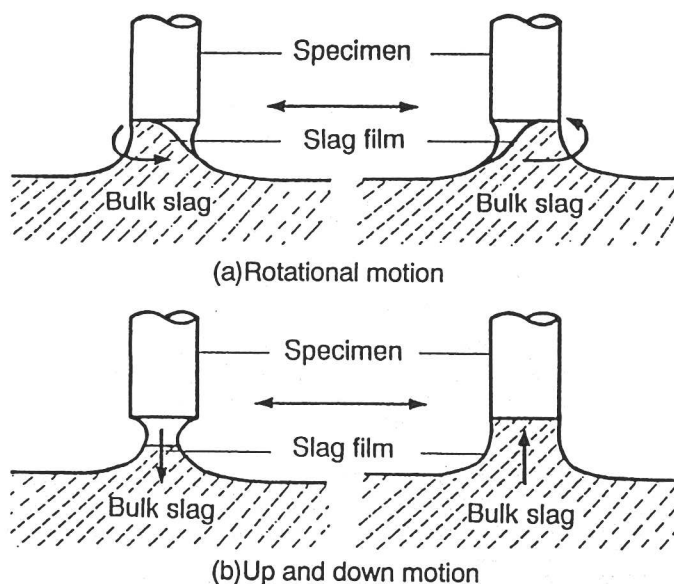


Fig.8 Typical slag film motions for a cylindrical specimen 6 mm dia. immersed in $\text{Fe}_t\text{O}-\text{SiO}_2$ slag during the initial stage (a) and the developed stage (b) of the local corrosion.

qualitatively from the standpoints of the Marangoni effect of the slag film induced by the dissolution of SiO_2 from the specimen into the film, and the wetting between the specimen and slag. However, in order to clarify the mechanism quantitatively, it is needed to obtain much more experimental evidences such as concentration change along the slag film surface, wetting between the slag and solid silica and hydrodynamic analysis of the film motion, etc.

5. Concluding Remarks

Direct observations performed by the authors have shown the real occurrences of the Marangoni effect in some high temperature melts even on the earth under normal gravity.

Slag film motions induced by the Marangoni effect in Chap.4 plays an essential role in the formation of the local corrosion of solid oxide.

Marangoni convection of liquid bridge due to temperature gradient in Chap.2 indicates that Marangoni convection can occur in the vicinity of solidifying liquid with free surface, for example, in the process of Czochralski method under normal gravity.

The Marangoni effect due to the change in applied potential in Chap.3 supports that the Marangoni flow can occur in the electrolytic processes using a liquid electrode[17].

Much more kinds of experiments and analyses on the Marangoni effect in high temperature melts may reveal additional phenomena or processes in which the Marangoni effect participates, and these, in turn, will lead to developments in the materials processings and also physical chemistry at high temperatures.

Reference

- 1) R. Brückner: *Glastech. Ber.*, 53(1980), 77.
- 2) K. Mukai: *Tetsu-to-Hagané*, 71(1985), 1435.
- 3) T. Nakamura, K. Yokoyama, F. Noguchi and K. Mukai: *CAMP-ISIJ*, 3(1990), 100.
- 4) T. Nakamura, K. Yokoyama, F. Noguchi and K. Mukai, *Molten Salt Chemistry and Technology Materials Science Forum*, ed. by M. Chemla and D. Devilliers, *Trans Tech Publications*, Switzerland, Vol. 73-75, 1991, 153.
- 5) K. Mukai, J. M. Toguri, I. Kodama and J. Yoshitomi: *Can. Metall.Q.*, 25(1986), 225.
- 6) K. Mukai, A. Iwata, T. Harada, J. Yoshitomi and S. Fujimoto: *J. Jpn. Inst. Met.*, 47(1983), 397.
- 7) K. Mukai, T. Nakano, T. Harada, J. Yoshitomi and S. Fujimoto: *Proc. 2nd Int. Symp. Metallurgical Slags and Fluxes*, *Met. Soc. AIME*, Pennsylvania, 1984, 207.
- 8) K. Mukai, T. Harada, T. Nakano and K. Hiragushi: *J. Jpn. Inst. Met.*, 49(1985), 1073.
- 9) K. Mukai, T. Harada, T. Nakano and K. Hiragushi: *J. Jpn. Inst. Met.*, 50(1986), 63.
- 10) T. Harada, S. Fujimoto, A. Iwata and K. Mukai: *J. Jpn. Inst. Met.*, 48(1984), 181.
- 11) Z. Yu, K. Yamashita and K. Mukai: *Synopsis of the 1991 Spring Meeting of Jpn. Inst. Met.*, (1991), 319, 320.
- 12) K. Morinaga, T. Yanagase, Y. Ohta and Y. Ueda, *TMS Paper Selection*, (1979), A-79-18.
- 13) N. Imaishi, S. Yasuhiro, T. Nakamura and K. Mukai: *Proc. 18th Int. Symp. on Space Technology and Science*, Kagoshima, Japan, 1992, to be published.
- 14) T. Nakamura, K. Yokoyama and K. Mukai: *Proc. 4th Int. Conference on Molten Slags and Fluxes*, Sendai, Japan, 1992, to be published.
- 15) M. Hino, T. Ejima and M. Kameda: *J. Jpn. Inst. Met.*, 31(1967), 113.
- 16) T. Ejima and M. Kameda: *J. Jpn. Inst. Met.*, 31(1967), 120.
- 17) Y. Ito: *Bulletin of Jpn. Inst. Met.*, 29(1990), 457.